Energy and Power Engineering, **2011, 3, 167-173**
doi:10.4236/epe.2011.32021 Published Online May 2011 (http://www.SciRP.org/journal/epe)

Numerical Research of Heat Transfer of Supercritical CO_2 in Channels

Lina Zhang[1], Minshan Liu[2], Qiwu Dong[2], Songwei Zhao[2]
[1]*School of Aeronautics Engineering*, *Zhengzhou Institute of Aeronautical Industry Management*, *Zhengzhou*, *China*
[2]*Thermal Energy Engineering Research Centre*, *Zhengzhou University*, *Zhengzhou*, *China*
E-mail: *lina*810619@163.*com*
Received December 17, 2010; *revised March* 18, 2011; *accepted April* 13, 2011

Abstract

With the worldwide development of nuclear power plant and requirement of saving energy and resource, high thermal efficiency and economical competitiveness are achieved by using supercritical CO_2 with special thermal properties and better flow and heat transfer characters. In this paper, heat transfer of supercritical CO_2 has been investigated in square and triangle array tube-bundle of cooled system in reactor using computational fluid dynamics (CFD) code FLUENT, and the basic knowledge of heat transfer of supercritical CO_2 and first experience of CFD simulation are obtained. The effect of mesh structures, turbulence models, as well as flow channel size is analyzed. The choice of turbulence model adopted in simulating supercritical CO_2 is recommended. Comparing the effect of heat transfer with supercritical CO_2 and supercritical water as cooled medium, the results show that the former was higher. The new idea is provided for choice of cooled medium and improving thermal efficiency this paper.

Keywords: Nuclear Power, Supercritical CO_2, Heat Transfer, Numerical Analysis

1. Introduction

Supercritical fluids are very popular in a number of industrial applications because of their special thermal properties, such as advanced water-cooled nuclear reactors, environmentally friendly air-conditioning and refrigeration systems and high pressure water oxidation plant for waste processing. Recently, carbon dioxide has been used frequently in experimental studies because of its lower critical pressure and temperature. A comprehensive understanding of the flow and heat transfer characteristic of supercritical fluid is essential for the purpose of performing accurate thermal-hydraulic predictions, which is important in supercritical light water reactor (SCLWR) design calculations. At the same time, heat transfer of supercritical fluids is studied by using computational fluid dynamics (CFD) codes for predicting the heat transfer coefficient and providing a better understanding of the heat transfer mechanism.

Kim *et al*. [1] researched the heat transfer of supercritical carbon dioxide flowing upward through tubes and a narrow annulus passage by experiments. S. M. Liao and T. S. Zhao [2] studied convective heat transfer to supercritical carbon dioxide in miniature tubes with diameters of 0.70, 1.40, and 2.16 mm. The results of experiments revealed that the buoyancy effects were significant for all the flow orientations, although Reynolds numbers were as high as 105. Chaobin Dang and Eiji Hihara [3] investigated experimentally heat transfer of supercritical carbon dioxide cooled in four horizontal cooling tubes with different inner diameters ranging from 1 to 6mm. M. Sharabi [4] *et al.* investigated the effect of different turbulent models on the simulation results of supercritical CO_2 in triangular and square channels.

The used turbulence models included RNG k-ε model and six kinds of low Reynolds number formulations. Pei-Xue Jiang *et al*. [5] investigated convection heat transfer of supercritical CO_2 in a 0.27 mm diameter vertical mini-tube experimentally and numerically. Lixin Cheng *et al*. [6] analyzed and compared many reports of heat transfer and pressure drop experimental data and correlations for supercritical CO_2 cooling in-macro- and micro-channels.

The large variation of the fluid physical properties of CO_2 at 8 MPa with temperature around the critical point influences heat transfer strongly as shown in **Figure 1**.

The temperature at which the specific heat at constant pressure attains a maximum value is called the pseudo critical temperature, T_{PC}. The important characteristics of fluids at supercritical pressure, which makes them very particular from the point of heat transfer, is that their specific heat vary rapidly with both pressure and temperature, as seen from **Figure 2**.

Although a large number of numerical studies on heat transfer of supercritical fluids have been carried out by various authors, these works are mostly concentrated to simple geometries which are usually circle tubes. The objective of this study is to figureure out the distinctive characteristics of supercritical heat transfer in various flow channels such as triangular tube and sub channels of rod bundles using the CFD code FLUENT.

2. Turbulent Models and Method of Solution

Three kinds of low Reynolds number turbulent models are considered including YS model, LS model and AKN model provided by FLUENT code. The low-Reynolds number turbulent models respond strongly to the effects of buoyancy and acceleration resulting from the sharp decrease in density with the increase of temperature due to heating and the subsequent redistribution of velocity in the near wall region, and exhibit severe localized deterioration of heat transfer. The model equations are as following:

Continuity

$$\frac{\partial \rho}{\partial t} + \nabla \cdot (\rho \boldsymbol{V}) = 0 \tag{1}$$

Momentum

$$\frac{\partial (\rho \boldsymbol{V})}{\partial t} + \nabla \cdot (\rho \boldsymbol{V}\boldsymbol{V}) = \nabla (\mu \nabla \boldsymbol{V}) - \nabla P + \rho \boldsymbol{g} \tag{2}$$

Energy

$$\frac{\partial (\rho T)}{\partial t} + \nabla \cdot (\rho \boldsymbol{V} T) = \nabla \left(\frac{\lambda}{C_p} \nabla T \right) \tag{3}$$

where ρ, μ, λ and CP are density, dynamic viscosity, thermal conductivity and specific heat for fluid, respectively, $\boldsymbol{V}$ and $\boldsymbol{g}$ are the dimensional velocity vector and gravity vector, t is time, and T is temperature.

Turbulent kinetic energy (k) [7]:

$$\frac{\partial (\rho k)}{\partial t} + \frac{\partial (\rho k u_i)}{\partial x_i} = \frac{\partial}{\partial x_j} \left[\left(\mu + \frac{\mu_t}{\sigma_k} \right) \frac{\partial k}{\partial x_j} \right] + G_k - \rho \varepsilon - \left| 2\mu \left(\frac{\partial k^{1/2}}{\partial n} \right)^2 \right| \tag{4}$$

Dissipation rate (ε):

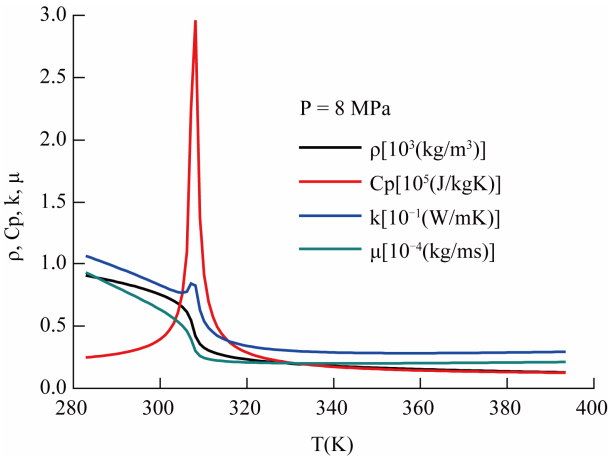

Figure 1. Properties near pseudo-critical temperature.

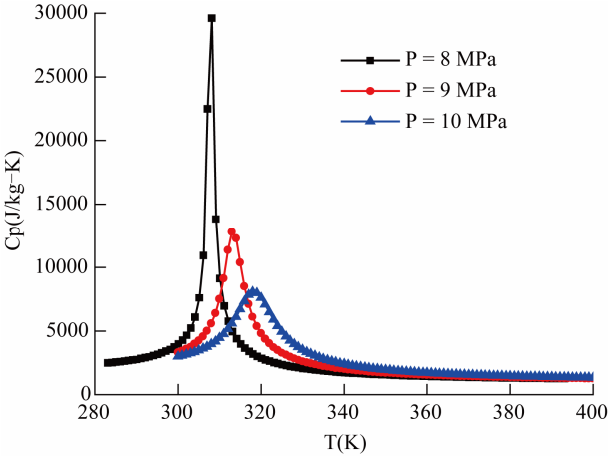

Figure 2. Specific heat with bulk fluid temperature.

$$\frac{\partial (\rho \varepsilon)}{\partial t} + \frac{\partial (\rho \varepsilon u_i)}{\partial x_i} = \frac{\partial}{\partial x_j} \left[\left(\mu + \frac{\mu_t}{\sigma_\varepsilon} \right) \frac{\partial \varepsilon}{\partial x_j} \right] + \frac{C_{1\varepsilon} \varepsilon}{k} G_k |f_1| - C_{2\varepsilon} \rho \frac{\varepsilon^2}{k} |f_2| + \left| 2 \frac{\mu \mu_t}{\rho} \left(\frac{\partial^2 u}{\partial n^2} \right)^2 \right| \tag{5}$$

where

$$\mu_t = C_\mu |f_\mu| \rho \frac{k^2}{\varepsilon} \tag{6}$$

The effect of gravity and buoyancy is considered. The QUICK scheme was used for approximating the convection terms in the momentum. Inlet is mass flow boundary condition, inlet fluid temperature and pressure are provided to define the inlet. Pressure outlet boundary condition is used for the outlet. SIMPLEC algorithm is adopted for pressure-velocity coupling, which is particularly recommended for the case of buoyant. The second order QUICK scheme is used for discretization of momentum, energy and turbulence equations. The carbon

dioxide is pressurized to 8 MPa. Inlet fluid temperature is 288.15 K.

3. Triangular Channel

To gather first experience in the application of CFD codes to supercritical fluids, a vertically oriented triangular channel was selected which studied experimental by Jong Kyu Kim, *et al*. [8]. The structure size, boundary conditions (symm represents symmetrical condition) and grid adopted in the simulation of the model is illustrated as **Figure 3**. Due to symmetry, only a half of the actual flow passage is modeled for the triangular channel. The hydraulic diameter is 9.8 mm and the heated length is 1.2 m. The sections before and after the heated section were 500 mm long (more than 40 d). Calculations with various size counts, which are 80 × (80 × 40), 100 × (100 × 50) and 120 × (120 × 60) in the axial directions and the OB side and OC side of the radial directions along the heated length, showed that the results were independent of the three kinds of size counts of grid. Therefore, the meshes with 100 size counts in the axial direction and (100 × 50) size counts in the radial direction were used. The convergence criteria required a decrease of at least six orders of magnitude for the residuals with no observable change in the surface temperatures for an additional 200 iterations.

Figure 4 shows the triangular duct wall temperatures predicted by the three kinds of low Reynolds number turbulent models under heat flux of 50 kW/m^2 and mass flux of 419 kg/(m^{2}s). In the study, computational simulations were compared with the selected experiments reported by Jong Kyu Kim *et al*. [8]. As can be seen, the simulations have the same trend with the experiment. The wall temperature appears a peak near Z/D_h equal to 20. Thereafter, the wall temperature decreases slightly as Z/D_h increases, as a result of the change in fluid transport properties. The results of different turbulent models are almost same. The AKN turbulence model over-predicts significantly turbulence reduction, and the result is same with S. He *et al*. [9].

In the later simulation of this paper, modeling results will be reported using the AKN because the results independent on the grid numbers can easily obtained according AKN turbulence model.

Figure 5 shows local Nusselt number variations in triangular tube along the flow direction, and the correlations and experimental data with the present simulated data are compared. The simulated data are very close to the experimental data during the heated section, and are in reasonably good agreement with the two correlations. Kransnoshchekov and Protopopov's and Jackson's correlations are based primarily on the forced convection at

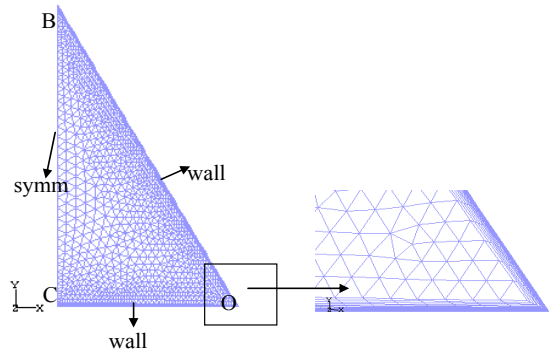

Figure 3. Grid and boundary conditions adopted for the triangular channel.

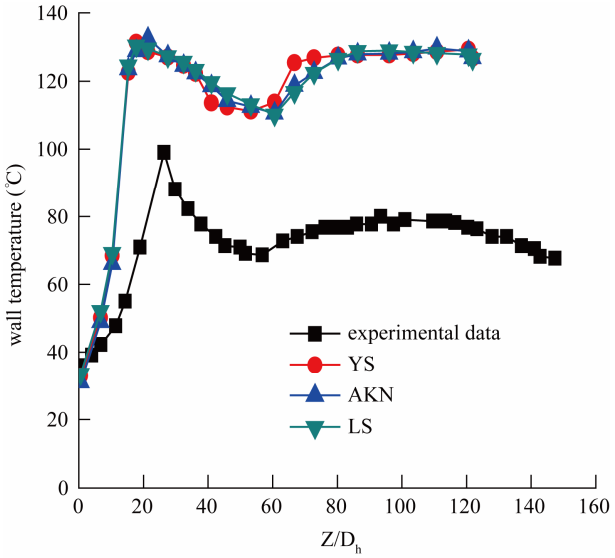

Figure 4. Wall temperature along the axial line C.

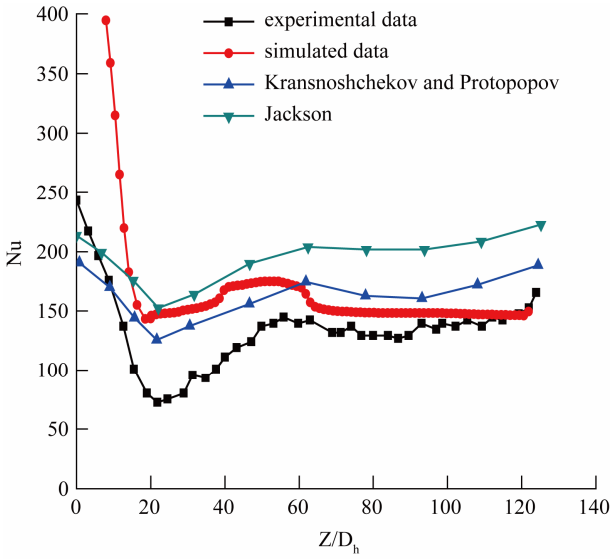

Figure 5. Local Nusselt number variations in the flow direction.

supercritical pressure. Other forced convection correlations for heating CO_2 in a vertical pipe have been proposed, but according to Jackson and Hall, Krasnoshchekov and Protopopov's correlation is the most accurate and is supported by the most experimental data [8].

The effect of mesh structures and turbulence models was studied. Based on a comparison of the numerical results with experimental data, the accuracy and applicability of turbulence models were assessed.

Figure 6 shows the wall temperature variations for the triangular channel in the axial direction at the different heat flux, with the mass flux is 314 kg/(m^{2}s). There is a peak in the temperature distribution, it shows the heat transfer deterioration. The deterioration takes place earlier at about Z/D_h equal to 10 under higher heat flux equal to 40 kW/m^2. The heat transfer deterioration takes place stronger under higher heat flux.

The distributions of Nusselt number along heated section under different heat flux are as shown in **Figure 7**. It is noted that the Nusselt number fluctuates to some extent. Nusselt number appears a peak under higher heat flux, and the heat transfer deterioration takes place earlier. Nusselt number appears two peaks under 20 kW/m^2.

4. Sub-Channels

In this section, sub-channels of both triangular-array and square-array rod bundles are taken, the structure and grid as indicated in **Figure 8**, and the simulated parameters are as **Table 1**.

Nusselt numbers for forced convection are calculated by using the Gnielinski correlation [10]:

$$Nu = \frac{(f/8)(\mathrm{Re}_b - 1000)\mathrm{Pr}_b}{1.07 + 12.7\sqrt{f/8}\left(\mathrm{Pr}_b^{2/3} - 1\right)} \quad (7)$$

$$f = \left[1.82\log_{10}(\mathrm{Re}_b) - 1.64\right]^{-2} \quad (8)$$

Figure 9 shows the Nusselt number of supercritical CO_2 and water in the square array rod bundles under pressure of 8 MPa and 25 MPa respectively. The mass flux and the heat flux of water are 740 kg/(m^{2}s) and 600 kW/m^2 respectively, and those of CO_2 are 300 kg/(m^{2}s) and 100 kW/m^2, respectively. The simulated data of supercritical water are cited from numerical analysis reported by X. Cheng *et al*. [11]. Supercritical CO_2 under far lower pressure, mass flux and heat flux, the Nusselt number is little lower than supercritical water. The effect of heat transfer with supercritical CO_2 is better than that of supercritical water.

Figure 10 and **Figure 11** show the effect of mass flux on Nusselt number as a function of fluid bulk temperature (T_b) of square and triangular array rod bundles, and

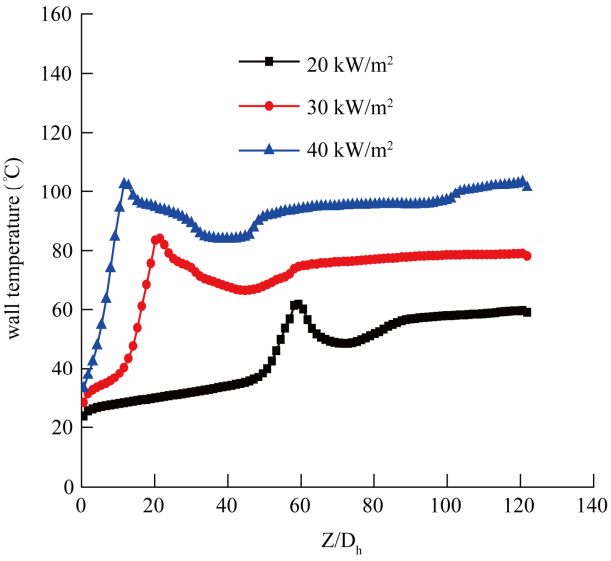

Figure 6. Wall temperature along the axial line C.

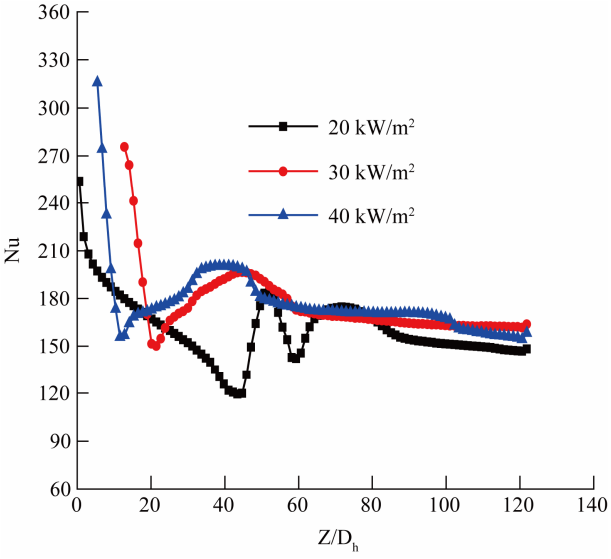

Figure 7. Local Nusselt number variations in the flow direction.

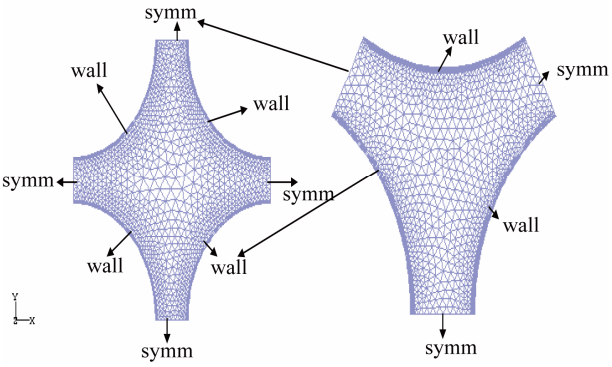

Figure 8. Grid structure and boundary conditions.

Table 1. Parameters for the sub channels simulation.

Parameters	Range
Rod bundle arrangement	Square, triangular
Rod diameter	8.0 mm
Pitch-to-diameter ratio	1.2
Pressure	8 MPa
Mass flux	200 - 300 kg/(m^{2}s)
Heat flux	60 - 100 kW/m^2
Fluid bulk temperature	280 - 350 K
Turbulence models	AKN

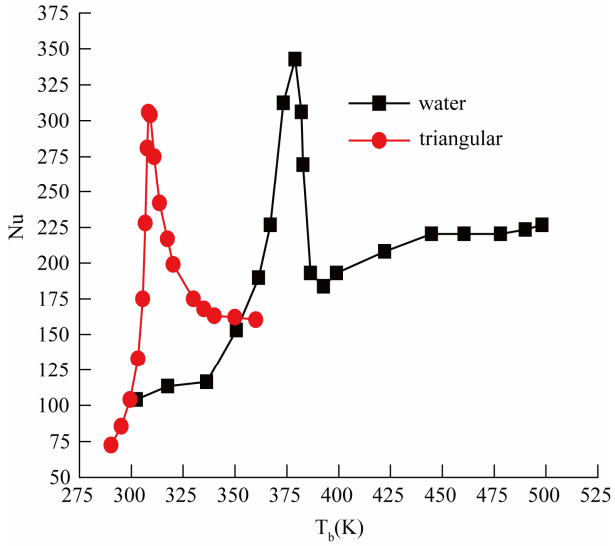

Figure 9. Variation of Nusselt number for supercritical CO_2 and water.

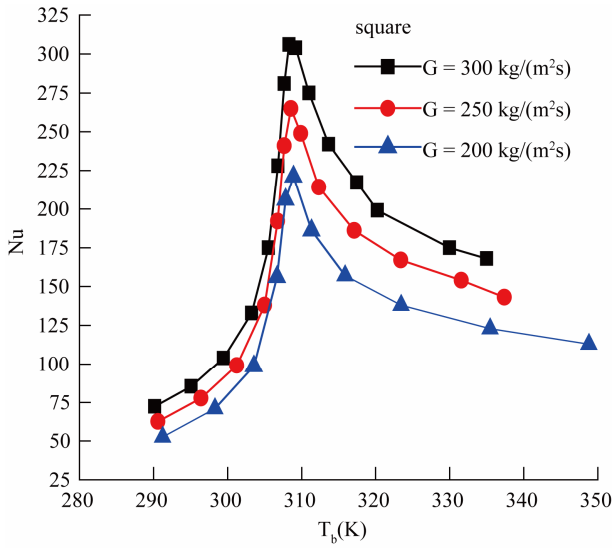

Figure 10. Mass flux effects on Nusselt number in square array rod bundle.

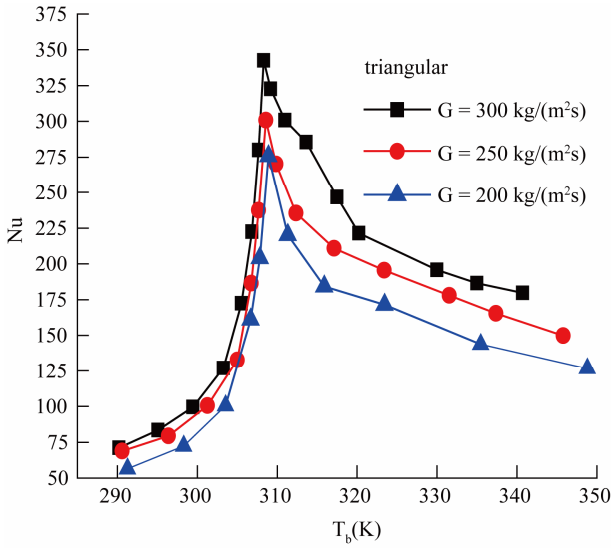

Figure 11. Mass flux effects on Nusselt number in triangular array rod bundle.

Tin equals to 288.15 K, heat flux is 100 kW/m^2. The mass flux effects Nusselt number significantly due to the increased Reynolds number. However, before the critical point, mass flux has less effect on heat transfer. The peak values increase with increasing mass flux. The peak of Nusselt number appears around the pseudocritical temperature. After the near-critical point region, the effect of mass flux on Nusselt number becomes more obvious.

Figure 12 shows the effect of heat flux on the Nusselt number as a function of bulk temperature in the square array rod bundles. Before the pseudocritical temperature, the Nusselt number under different heat flux is nearly same. With the increasing bulk temperature, the variety becomes more obvious. Especially under lower heat flux, the Nusselt number decreases significantly.

Figure 13 shows the comparison between the square lattice and triangular lattice of Nusselt number along bulk temperature with the heat flux 100 kW/m^2. The heat transfer is enhanced in the triangular lattice at pseudocritical temperature and got cross that temperature, and the reason is that the degree of turbulence increases because of the change of structure of flow channels.

5. Conclusions

Heat transfer of supercritical CO_2 has been investigated in various flow channels. Three kinds of low Reynolds number turbulent models are adopted to analyze the effect on the wall temperature of the triangle channels, and the results show that difference under different turbulent models is rather small, and then AKN turbulent model are chosen.

In triangular channels, the wall temperature increases

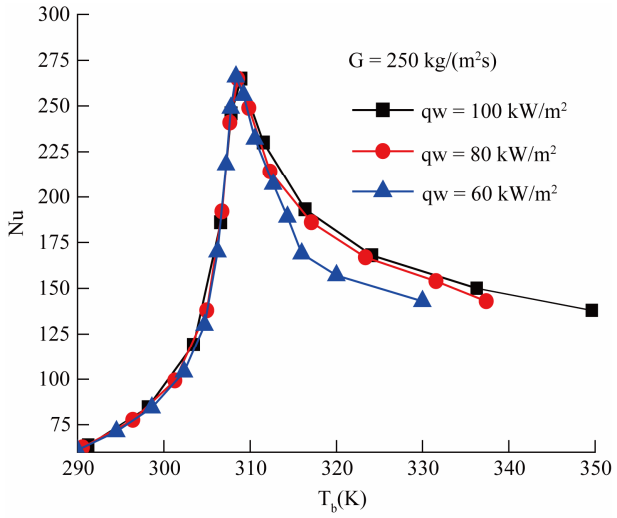

Figure 12. Heat flux effects on Nusselt number of square array rod bundle.

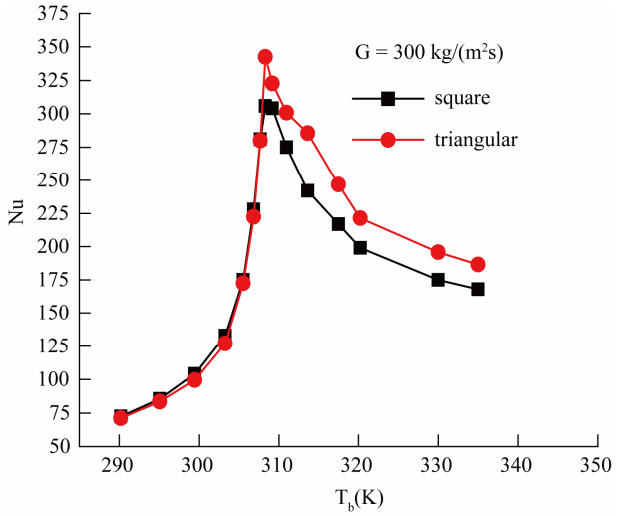

Figure 13. Comparison of square array rod bundle with triangular array rod bundle.

with increasing heat flux. The heat transfer deterioration takes place earlier with higher heat flux, whereas Nusselt number appeared two peaks under lower heat flux.

The heat transfer effect of supercritical CO_2 is better than that of supercritical water. The effect of mass flux on Nusselt number is more obvious than heat flux. The Nusselt number is higher under larger mass flux, especially across the pseudocritical temperature. The heat transfer effect with triangular array rod bundles is better than that of square array rod bundles under the same heat flux and mass flux.

6. Acknowledgments

This work was supported by the National Natural Science Foundation of China (51076145). The authors would like to thank teachers of Thermal Energy Engineering Research Center of Zhengzhou University.

7. References

[1] K. Hyungrae, Y. K. Hwan, J. H. Song *et al*., "Heat Transfer to Supercritical Pressure Carbon Dioxide Flowing Upward through Tubes and a Narrow Annulus Passage," *Progress in Nuclear Energy*, Vol. 50, No. 2-6, 2008, pp. 518-525. doi:10.1016/j.pnucene.2007.11.065

[2] S. M. Liao and T. S. Zhao, "An Experimental Investigation of Convection Heat Transfer to supercritical Carbon Dioxide in Miniature Tubes," *International Journal of Heat and Mass Transfer*, Vol. 45, No. 25, 2002, pp. 5025-5034. doi:10.1016/S0017-9310(02)00206-5

[3] C. B. Danga and E. J. Hihara, "In-Tube Cooling Heat Transfer of Supercritical Carbon Dioxide. Part 1: Experimental Measurement," *International Journal of Refrigeration*, Vol. 27, No. 7, 2004, pp. 736-747. doi:10.1016/j.ijrefrig.2004.04.018

[4] M. Sharabi, W. Ambrosini, S. He *et al*., "Prediction of Turbulent Convective Heat Transfer to a Fluid at Supercritical Pressure in Square and Triangular Channels," *Annals of Nuclear Energy*, Vol. 35, No. 6, 2008, pp. 993-1005. doi:10.1016/j.anucene.2007.11.006

[5] P. X. Jiang, Y. Zhang and R. F. Shi, "Experimental and Numerical Investigation of Convection Heat Transfer of CO_2 at Supercritical Pressures in a Vertical Mini-Tube," *International Journal of Heat and Mass Transfer*, Vol. 51, No. 11-12, 2008, pp. 3052-3056. doi:10.1016/j.ijheatmasstransfer.2007.09.008

[6] L. X. Cheng, G. Ribatskia and J. R. Thome, "Analysis of Supercritical CO_2 Cooling in Macro- and Micro-Channels," *International Journal of Refrigeration*, Vol. 31, No. 8, 2008, pp. 1-16. doi:10.1016/j.ijrefrig.2008.01.010

[7] M. van der Kraan, M. M. W. Peeters, M. V. Fernandez Cid, G. F. Woerlee, W. J. T. Veugelers and G. J. Witkamp, "The Influence of Variable Physical Properties and Buoyancy on Heat Exchanger Design for Near- and Supercritical Conditions," *The Journal of Supercritical Fluids*, Vol. 34, No. 1, 2005, pp. 99-105. doi:10.1016/j.supflu.2004.10.007

[8] J. K. Kim, H. K. Jeon and J. S. Lee, "Wall Temperature Measurement and Heat Transfer Correlation of Turbulent Supercritical Carbon Dioxide Flow in Vrtical Circular/Non-Circular Tubes," *Nuclear Engineering and Design*, Vol. 237, No. 15-17, 2007, pp. 1795-1802. doi:10.1016/j.nucengdes.2007.02.017

[9] S. He, W. S. Kim and J. H. Bae, "Assessment of Performance of Turbulence Models in Predicting Supercritical Pressure Heat Transfer in a Vertical Tube," *International Journal of Heat and Mass Transfer*, Vol. 51, No. 19-20, 2008, pp. 4659-4675. doi:10.1016/j.ijheatmasstransfer.2007.12.028

[10] V. Gnielinski, "New Equations for Heat and Mass Transfer in Turbulent Pipe and Channel Flow," *International Chemical Engineering*, Vol. 16, No. 2, 1976, pp. 359-68.

[11] X. Cheng, B. Kuang and Y. H. Yang, "Numerical Analysis of Heat Transfer in Supercritical Water Cooled Flow Channels," *Nuclear Engineering and Design*, Vol. 237, No. 3, 2007, pp. 240-252. doi:10.1016/j.nucengdes.2006.06.011

